

Molecular Orientation Control of Liquid Crystal Organic Semiconductor for High Performance Organic Field Effect Transistors

Moon Jong Han[†], Don-Wook Lee[‡], Eun Kyung Lee[‡], Joo-Young Kim[‡], Ji Young Jung[‡],
Hyunbum Kang[‡], Hyungju Ahn[§], Tae Joo Shin^{||}, Dong Ki Yoon^{†,⊥,*}, and Jeong-Il Park^{‡,*}

*To whom correspondence should be addressed.

E-mail: nandk@kaist.ac.kr and jeong.park@samsung.com

[†]Graduate School of Nanoscience and Technology, Korea Advanced Institute of Science and Technology (KAIST), Daejeon 34141, Republic of Korea

[‡]Material Research Center, Samsung Advanced Institute of Technology, Samsung Electronics Co., Ltd., Samsung-ro 130, Yongtong-gu, Suwon-si, Gyeonggi-do 16678, Republic of Korea

[§]Pohang Accelerator Laboratory, POSTECH, Pohang 37673, Republic of Korea

^{||}UNIST Central Research Facilities & School of Natural Science, Ulsan National Institute of Science and Technology (UNIST), Ulsan 44919, Republic of Korea

[⊥]Department of Chemistry and KINC, Korea Advanced Institute of Science and Technology (KAIST), Daejeon, 34141, Republic of Korea

Table of Contents

S1. Synthetic route of C12-Th-DBTTT.

S2. Polarized optical microscope images of C12-Th-DBTTT.

S3. Optical microscopy and atomic force microscopy images of thermally deposited C12-Th-DBTTT films at 30 °C and followed by 200 °C thermal annealing.

S4. Optical microscope (OM) and atomic force microscope (AFM) images of thermally deposited C12-Th-DBTTT films at different substrate temperature.

S5. Atomic force microscopy (AFM) measurements of thermally deposited C12-Th-DBTTT films at 165 °C followed by thermal annealing.

S6. 2D-GIXD patterns of polycrystalline C12-Th-DBTTT powder sample with lattice parameters.

S7. 2D-GIXD patterns of polycrystalline C12-Th-DBTTT films as thermally deposited at 165 °C followed by thermal annealing.

S8. Herringbone structure of C12-Th-DBTTT with *ab* plane.

S9. 1D plots extracted from 2D GIXD measurement of solution sheared films with different thermal annealing temperature.

S10. Output curves of C12-Th-DBTTT films as thermally deposited and solution sheared at 165 °C and post thermal annealing.

S11. Electrical characterization of C12-Th-DBTTT film as thermally deposited at 30 °C and followed by 200 °C thermal annealing.

S12. Molecular rearrangement characteristics depending on film fabrication temperature.

S13. Contact resistance of OTFTs based on C12-Th-DBTTT films.

S14. Transfer curve of C12-Th-DBTTT-based OTFT at 350 °C.

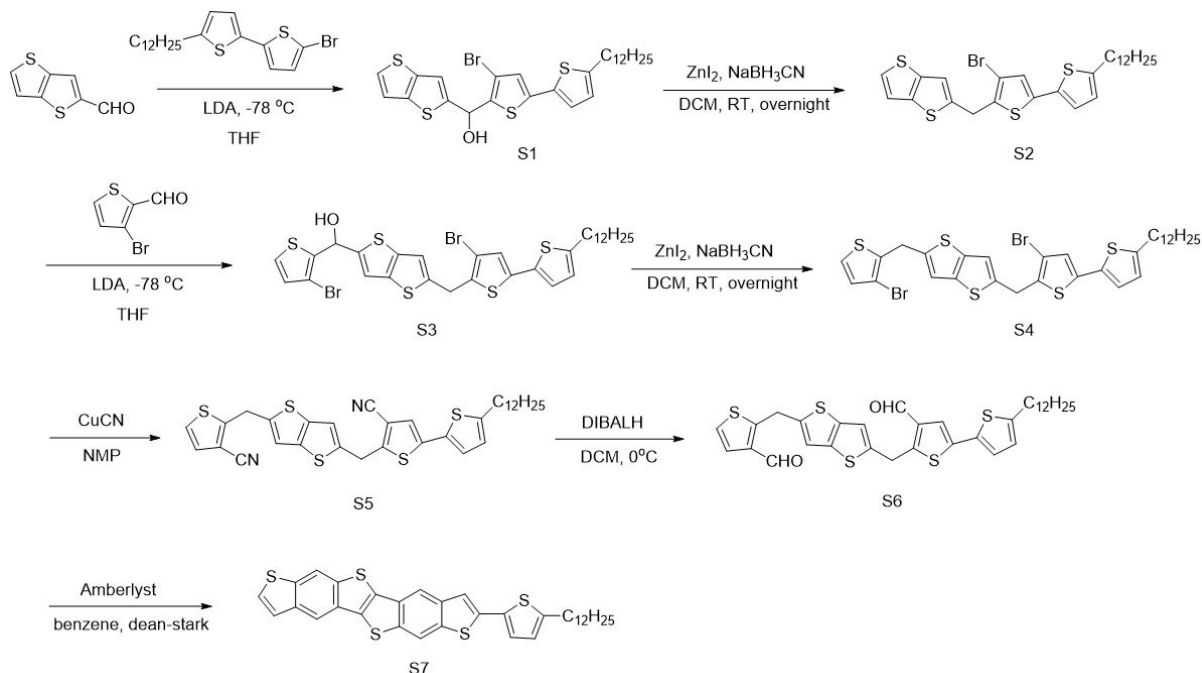


Figure S1. Synthetic route of C12-Th-DBTTT.

(1) Synthesis:

Compound S1: To a chilled (-78 °C) solution of 5-bromo-5'-dodecyl-2,2'-bithiophene (10g, 24.18 mmol) in dry THF (500 mL) was added LDA (2.0 M in THF, 14.51 mL, 1.2 eq.) and the reaction mixture was vigorously stirred for 2 hours at -78°C, and then thieno[3,2-b]thiophene-2-carbaldehyde (4.07 g, 24.18 mmol) was added. The reaction mixture was stirred overnight, and then quenched with sat. ammonium chloride solution. The THF solution was diluted with ethyl acetate and washed with water several times. The organic layer was dried over magnesium sulfate and evaporated to give a brown solid. The product was filtered through silica pad (ethyl acetate/hexane=1/5) and re-crystallized from diethyl ether to yield compound S1 (10.75 g, 76.5 %) as an ivory solid. ¹H-NMR (500 MHz, CDCl₃): δ 7.35 (d, 1H), 7.22 (d, 1H), 6.96 (d, 1H), 6.93 (s, 1H), 6.67 (d, 1H), 6.39 (d, 1H), 2.78 (t, 2H), 2.76 (s, 1H), 1.66 (t, 2H), 1.28 (m, 18H), 0.88 (t, 3H); ¹³C-NMR (75.5 MHz, CDCl₃): 147.35, 146.74, 139.16, 138.78, 138.42, 138.22, 133.18, 127.30, 124.98, 124.93, 124.16, 119.61, 117.59, 108.76, 68.69, 31.92, 31.54, 30.16, 29.96, 29.63, 29.53, 29.36, 29.34, 29.04, 22.70, 14.13

Compound S2: To a stirred turbid solution of compound S1 (10.71 g, 18.41 mmol) in dichloromethane (600mL), zinc (II) iodide (9.4 g, 29.46 mmol) and sodium cyanoborohydride (8.1 g, 128.88 mmol) were added slowly at room temperature. The reaction mixture was stirred 24 h, and then was filtered through Celite pad to remove the precipitate. The organic layer was washed successively with sat. ammonium chloride solution and brine. The resulting solution was dried over magnesium sulfate and evaporated to give a crude solid. The solid was re-crystallized from ether/hexane to yield compound S2 (10 g, 96%) as a pale pink solid. ¹H-NMR (500 MHz, CDCl₃):

δ 7.30 (d, 1H), 7.18 (d, 1H), 7.01 (s, 1H), 6.92 (s, 1H), 6.90 (d, 1H), 6.64 (d, 1H), 4.32 (s, 2H), 2.76 (t, 2H), 1.65 (t, 2H), 1.29 (m, 18H), 0.88 (t, 3H) ; ^{13}C -NMR (75.5 MHz, CDCl_3): 146.27, 143.62, 138.63, 138.34, 136.82, 135.13, 133.42, 126.27, 125.03, 124.81, 123.74, 119.46, 117.91, 109.56, 31.92, 31.55, 30.79, 30.14, 29.66, 29.63, 29.53, 29.35, 29.34, 29.03, 22.70, 14.13

Compound S3: To a chilled (-78°C) solution of 2-((4-bromo-5'-dodecyl-[2,2'-bithiophen]-5-yl)methyl)thieno[3,2-b]thiophene (10g, 17.68 mmol) in dry THF (500 mL) was added LDA (2.0 M in THF, 10.61 mL, 1.2 eq.) and the reaction mixture was vigorously stirred for 2 hours at -78°C , and then 3-bromothiophene-2-carbaldehyde (4.05 g, 21.21 mmol) was added. The reaction mixture was stirred overnight, and then quenched with sat. ammonium chloride solution. The THF solution was diluted with ethyl acetate and washed with water several times. The organic layer was dried over magnesium sulfate and evaporated to give a brown solid. The product was filtered through silica pad (ethyl acetate/hexane=1/5) and re-crystallized from diethyl ether to yield compound S3 (7.2 g, 54 %) as an ivory solid. ^1H -NMR (500 MHz, CDCl_3): δ 7.30 (d, 1H), 7.13 (s, 1H), 7.05 (s, 1H), 6.95 (d, 1H), 6.91 (s, 1H), 6.90 (d, 1H), 6.64 (d, 1H), 6.39 (d, 1H), 4.30 (s, 2H), 2.75 (t, 2H), 2.72 (s, 1H), 1.65 (t, 2H), 1.28 (m, 18H), 0.88 (t, 3H) ; ^{13}C -NMR (75.5 MHz, CDCl_3): 146.51, 146.31, 143.70, 141.13, 138.57, 137.39, 136.86, 134.96, 133.39, 132.04, 130.06, 125.70, 125.04, 124.82, 123.77, 118.14, 117.77, 109.61, 108.63, 68.65, 31.93, 31.56, 30.71, 30.15, 29.66, 29.64, 29.54, 29.36, 29.34, 29.04, 22.70, 14.21, 14.14

Compound S4: To a stirred turbid solution of compound S3 (7.2 g, 9.51 mmol) in dichloromethane (500mL), zinc (II) iodide (4.86 g, 15.22 mmol) and sodium cyanoborohydride (4.2 g, 66.6 mmol) were added slowly at room temperature. The reaction mixture was stirred 24 h, and then was filtered through Celite pad to remove the precipitate. The organic layer was washed successively with sat. ammonium chloride solution and brine. The resulting solution was dried over magnesium sulfate and evaporated to give a crude solid. The solid was re-crystallized from ether/hexane to yield compound S4 (4.78 g, 68 %) as a pale pink solid. ^1H -NMR (500 MHz, CDCl_3): δ 7.17 (d, 1H), 7.01 (s, 1H), 6.99 (s, 1H), 6.94 (d, 1H), 6.91 (s, 1H), 6.89(d, 1H), 6.64 (d, 1H), 4.33 (s, 2H), 4.29 (s, 2H), 2.76 (t, 2H), 1.64 (t, 2H), 1.29 (m, 18H), 0.88 (t, 3H); ^{13}C -NMR (75.5 MHz, CDCl_3): 146.22, 142.78, 142.50, 137.60, 137.57, 137.12, 136.77, 135.20, 133.42, 129.96, 125.00, 124.79, 124.39, 123.71, 118.02, 117.95, 109.56, 109.48, 31.92, 31.54, 30.64, 30.49, 30.14, 29.65, 29.63, 29.53, 29.35, 29.33, 29.03, 22.69, 14.13

Compound S5: A solution of Compound S4 (4.78 g, 6.45 mmol) in N-methylpyrrolidone (75 mL) was added copper cyanide (2.31g, 25.81 mmol) and vigorously stirred for 1 hour in microwave at the 180°C . The reaction mixture was cooled, and then quenched with 1N HCl solution. The sticky solid was filtered from the solution. Then, the resulting solid was solved with chloroform and washed with water several times. The organic layer was dried over magnesium sulfate and was evaporated to give a solid. The product was purified by silica column chromatography (ethyl acetate/hexane=1/5) and re-crystallized from ether to yield compound S5 (2.85 g, 67 %) as an yellow solid. ^1H -NMR (500 MHz, CDCl_3): δ 7.23 (d, 1H), 7.16 (d, 1H), 7.09 (s, 1H), 7.08 (s, 1H), 7.06 (s, 1H), 6.93 (d, 1H), 6.66 (d, 1H), 4.55 (s, 2H), 4.51 (s, 2H), 2.77 (t, 2H), 1.65 (t, 2H), 1.28 (m, 18H), 0.88 (t, 3H) ; ^{13}C -NMR (75.5 MHz, CDCl_3): 154.17, 151.90, 147.28, 141.87, 141.68, 138.21, 138.03, 132.18, 128.44, 125.48, 125.00, 124.85, 122.60, 118.68, 118.64, 109.08, 108.91, 31.92, 31.53, 30.65, 30.48, 30.14, 29.66, 29.53, 29.35, 29.32, 29.03, 22.70, 14.14

Compound S6: Diisobutylaluminium hydride (1.0 M in cyclohexane, 10.81 mL, 10.81 mmol) was added slowly to a chilled (0 °C) solution of Compound S5 (2.85 g, 4.5 mmol) in dry dichloromethane (300 mL) and vigorously stirred for 4 hour at room temperature. The reaction mixture was quenched with sat. ammonium chloride solution. The resulting solution was diluted with dichloromethane and washed with water several times. The organic layer was dried over magnesium sulfate and was evaporated to give a solid. The product was purified by silica column chromatography (ethyl acetate/hexane=1/5) and re-crystallized from ether to yield compound S6 (1.76 g, 61 %) as an ivory solid. . $^1\text{H-NMR}$ (500 MHz, CDCl_3): δ 10.08 (s, 1H), 10.03 (s, 1H), 7.41 (d, 1H), 7.34 (s, 1H), 7.17 (d, 1H), 7.04 (s, 1H), 7.02 (s, 1H), 6.93 (d, 1H), 6.66 (d, 1H), 4.75 (s, 2H), 4.72 (s, 2H), 2.77 (t, 2H), 1.66 (t, 2H), 1.28 (m, 18H), 0.88 (t, 3H) ; $^{13}\text{C-NMR}$ (75.5 MHz, CDCl_3): 184.68, 184.39, 128.28, 124.87, 124.34, 124.06, 122.45, 118.44, 118.35, 31.92, 31.55, 30.15, 29.63, 29.53, 29.48, 29.43, 29.34, 29.04, 22.70, 14.13

Compound C12-Th-DBTTT (S7): To a stirred solution of compound S6 (1.76 g, 2.75 mmol) in dry benzene (20 mL), amberlyst 15 (3.5 g) was added under N_2 atmosphere. The resulting solution was refluxed overnight, and then chilled to room temperature. The floating product was filtered to yield a grey solid, which was further purified by sublimation for device fabrication. HRMS (m/z): $[\text{M}]^+$ calcd for $\text{C}_{34}\text{H}_{34}\text{S}_5$ 602.29; found

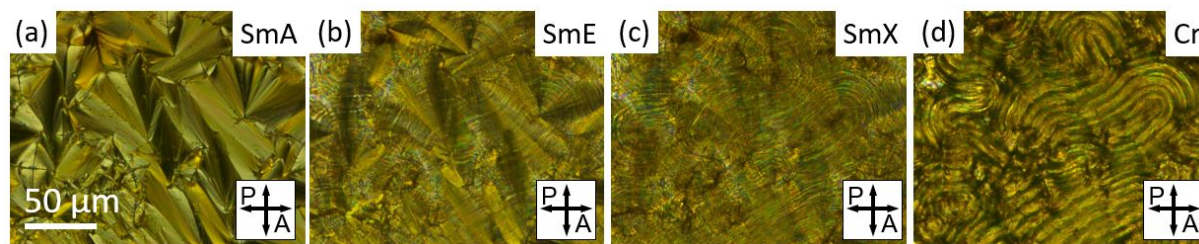


Figure S2. Polarized optical microscope images of (a) SmA (380 °C), (b) SmE (260 °C), (c) SmX (180 °C), and (d) crystal (45 °C). Each liquid crystal phases were measured by POM, in which the samples were prepared by sandwich cells with 5 μm gap, consisting of two pristine glass substrates.

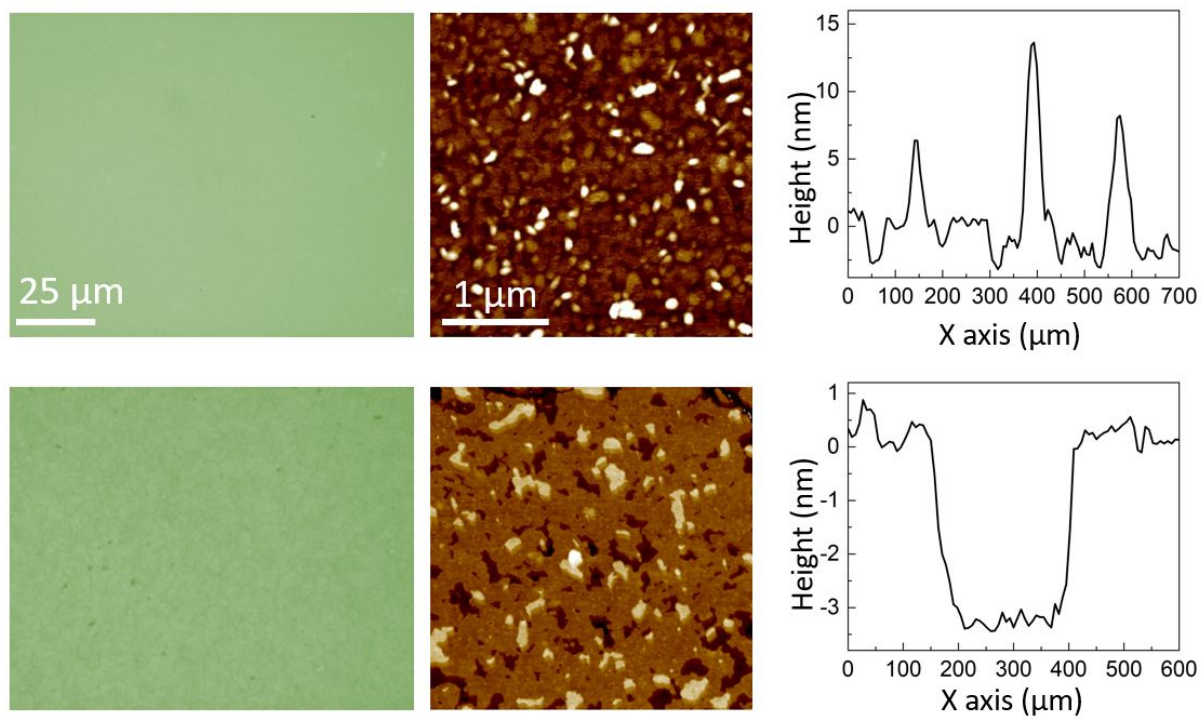


Figure S3. Optical microscopy and atomic force microscopy images of thermally deposited C12-Th-DBTTT films at 30 °C and followed by 200 °C thermal annealing.

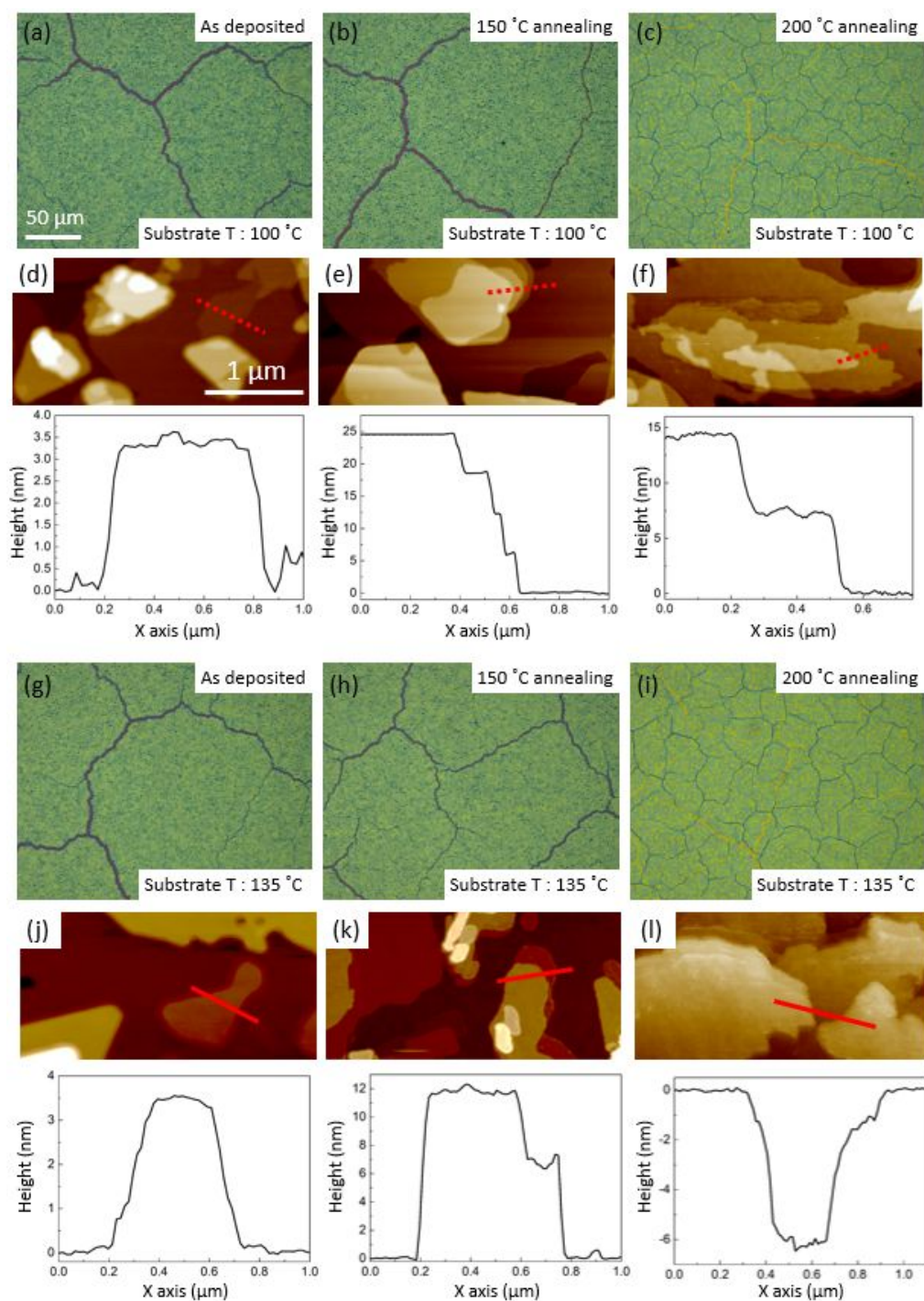


Figure S4. Optical microscope (OM) and atomic force microscope (AFM) images of thermally deposited C12-Th-DBTTT films at different substrate temperature, such as (a-f) 100 °C and (g-l) 135 °C with thermal annealing treatment temperature.

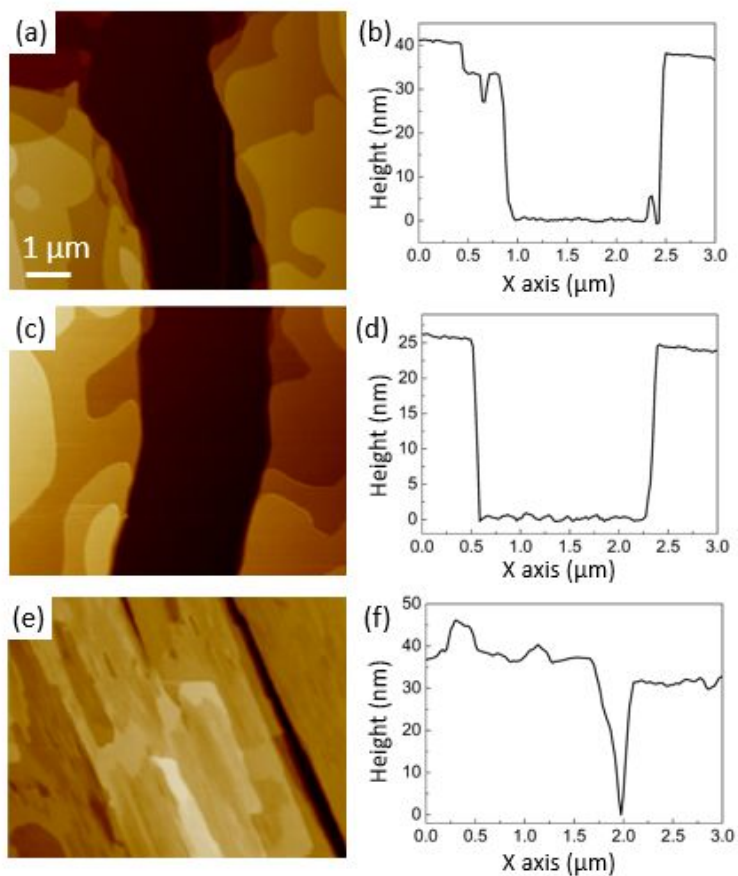


Figure S5. Atomic force microscopy (AFM) measurements of thermally deposited C12-Th-DBTTT films at 165 °C followed by thermal annealing. The deposited sample (a) was treated by thermal annealing at (c) 150 °C and (e) 200 °C for 5 min. Each samples showing cracks were characterized by height profiles as shown in (b,d,f).

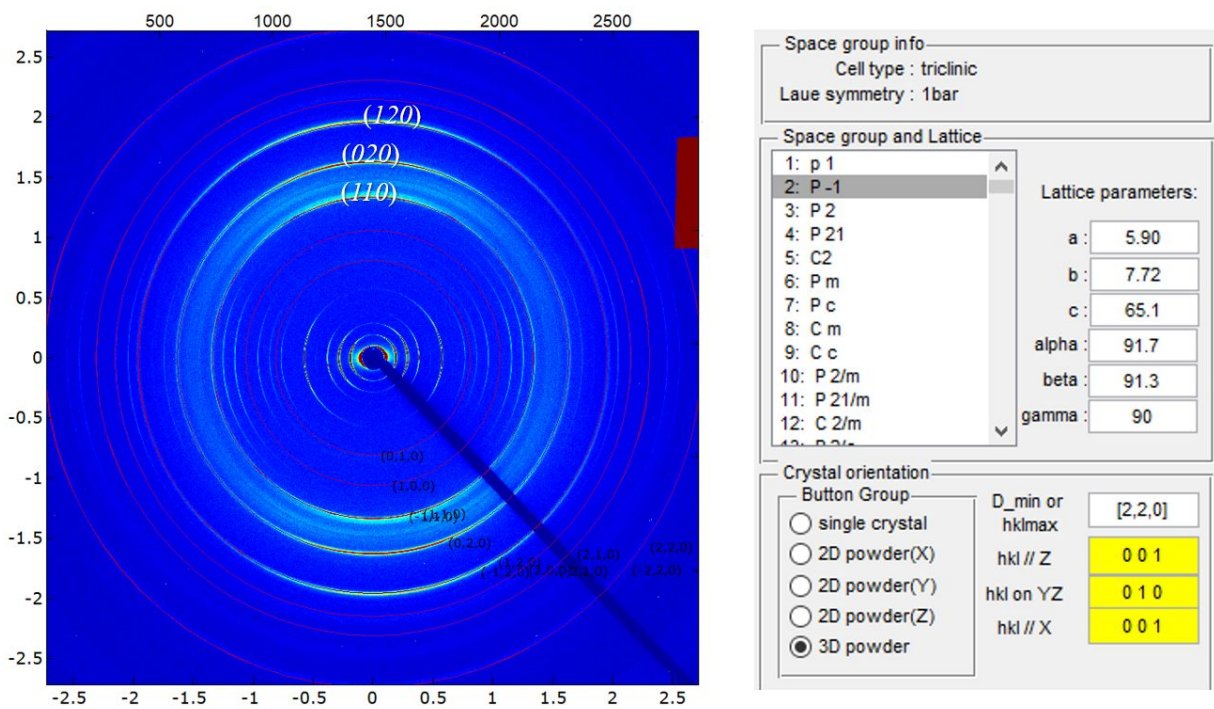


Figure S6. 2D-GIXD patterns of polycrystalline C12-Th-DBTTT powder sample with lattice parameters.

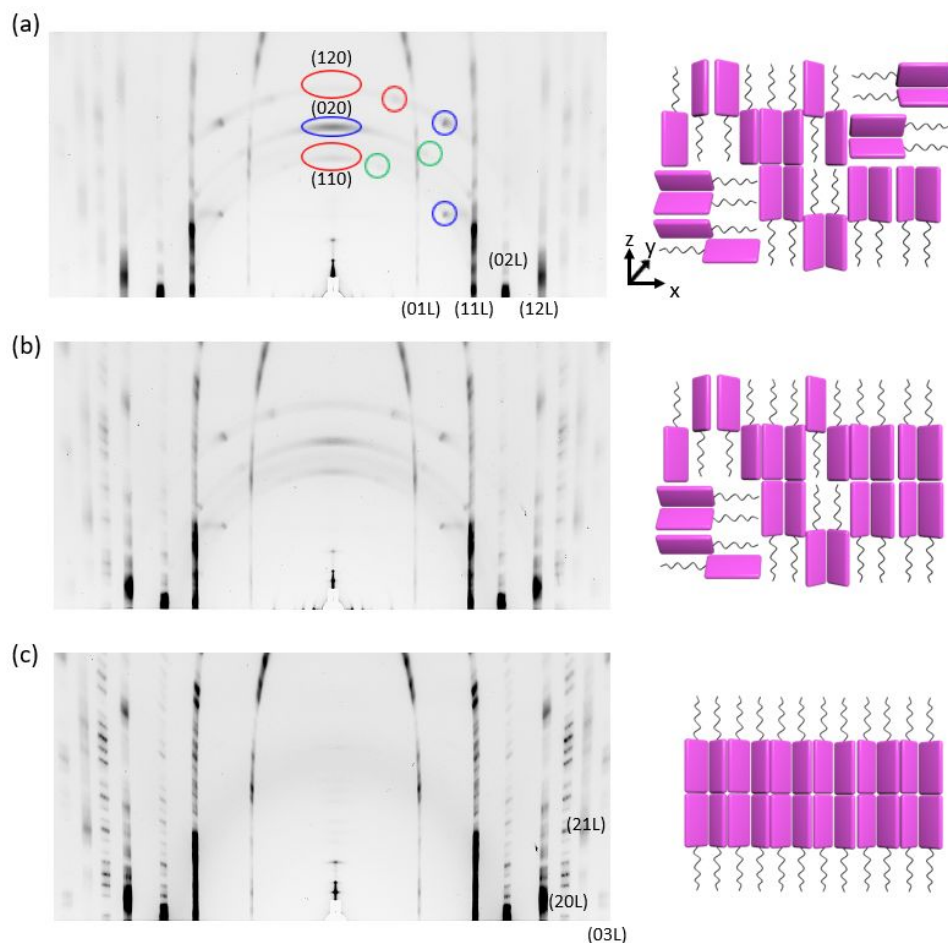


Figure S7. 2D-GIXD patterns of polycrystalline C12-Th-DBTTT films as thermally deposited at 165 °C followed by thermal annealing. (a) As deposited and (b) annealed at 150 °C and (c) 200 °C. For major polymorph 1, the (001) diffraction was parallel to the substrate, exhibiting edge-on orientation, whose lattice parameters were $a = 5.90 \text{ \AA}$, $b = 7.72 \text{ \AA}$, $c = 32.6 \text{ \AA}$, $\alpha = 92.1^\circ$, $\beta = 94.7^\circ$, $\gamma = 90^\circ$. The other three minor polymorphs 2, 3, and 4 showed face-on orientation, in which the (010), (110), and (120) diffraction were parallel to the substrate, corresponding to the blue, red, and green circles, respectively.

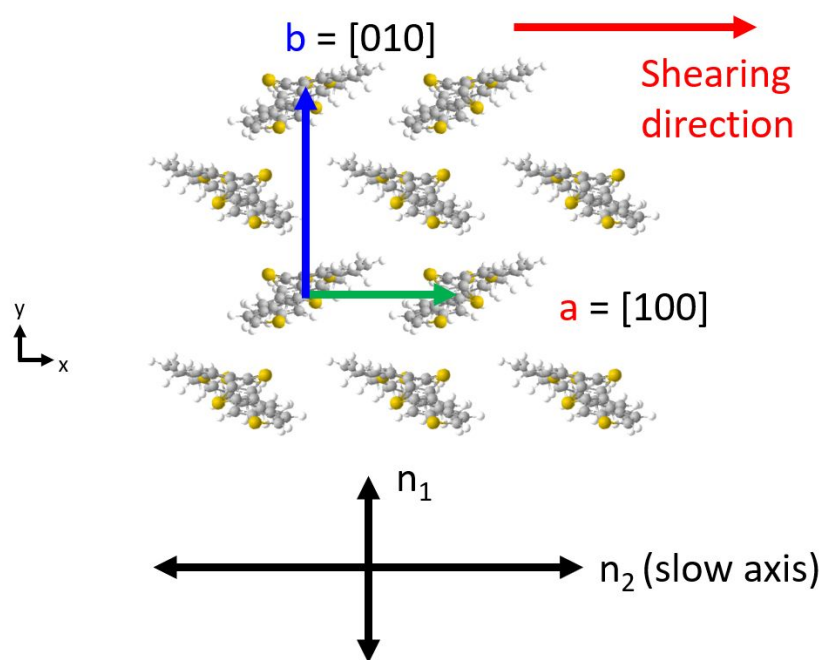


Figure S8. Herringbone structure of C12-Th-DBTTT with ab plane. The view perpendicular to the ab plane of C12-Th-DBTTT demonstrates the relationship between crystallographic axes a , b and fast and slow axis n_1 , n_2 with solution shearing direction.

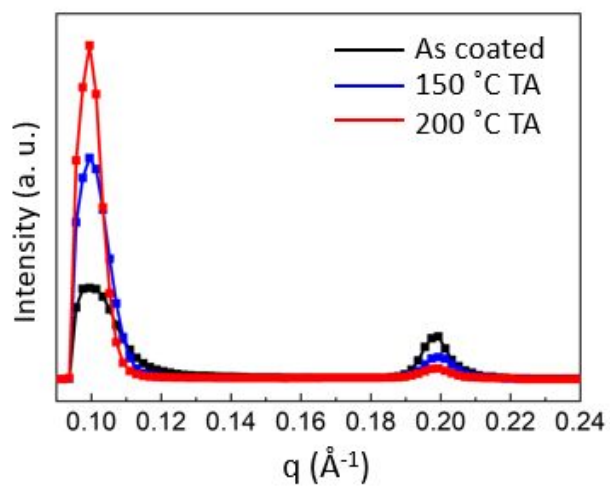


Figure S9. 1D plots extracted from 2D GIXD measurement of solution sheared films with different thermal annealing temperature. Out-of-plane small-angle XRD results of aligned C12-Th-DBTTT films with 150 °C and 200 °C thermal annealing.

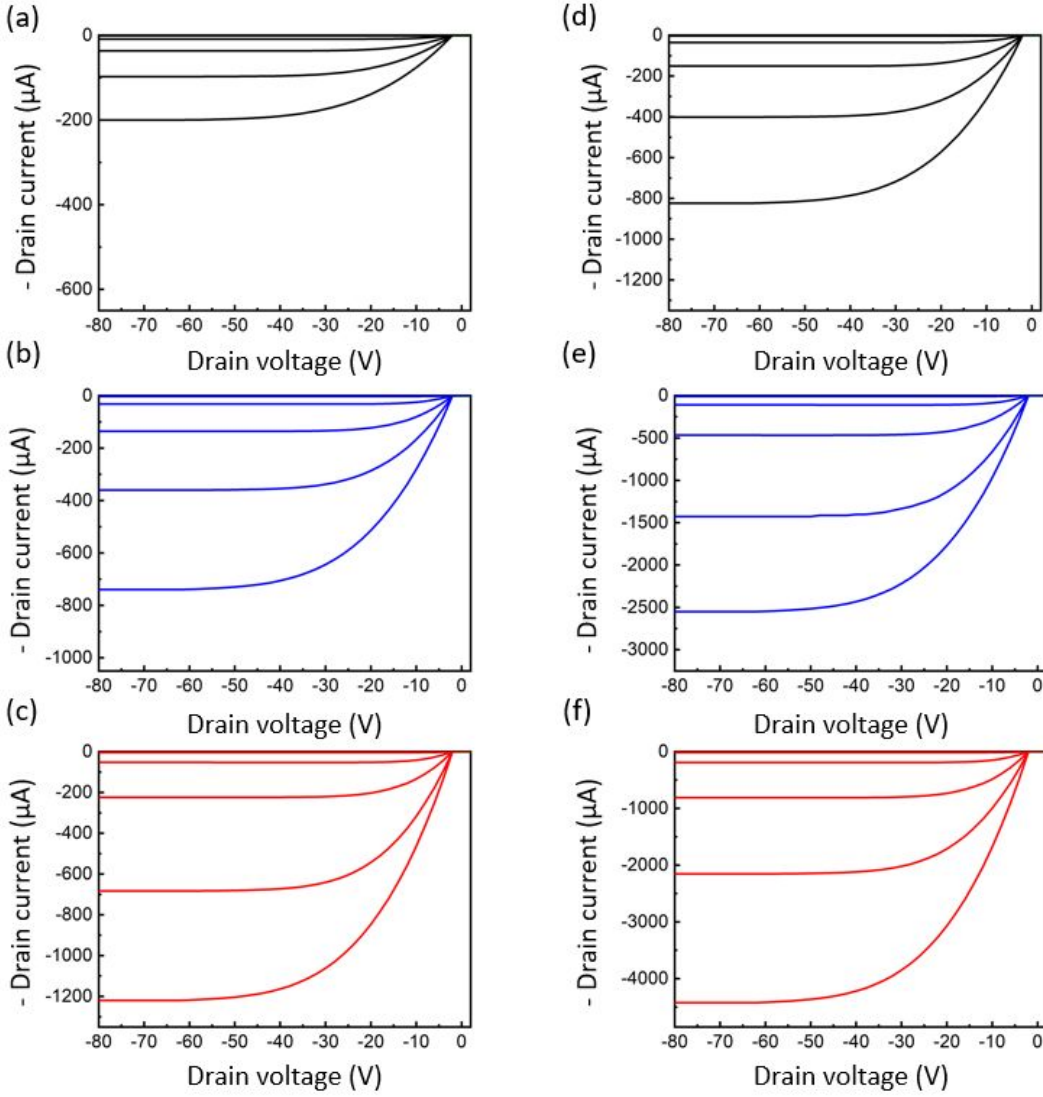


Figure S10. Output curves of C12-Th-DBTTT films as thermally deposited and solution sheared at 165 °C and post thermal annealing. (a,b,c) polycrystalline films by thermal evaporation and (d,e,f) highly oriented films by solution shearing (a,d) as deposited at 165 °C and (b,e) followed by 150 °C and (c,f) 200 °C thermal annealing (TA). In the output curves, the V_G range was from 0 to – 60V with – 10 V steps.

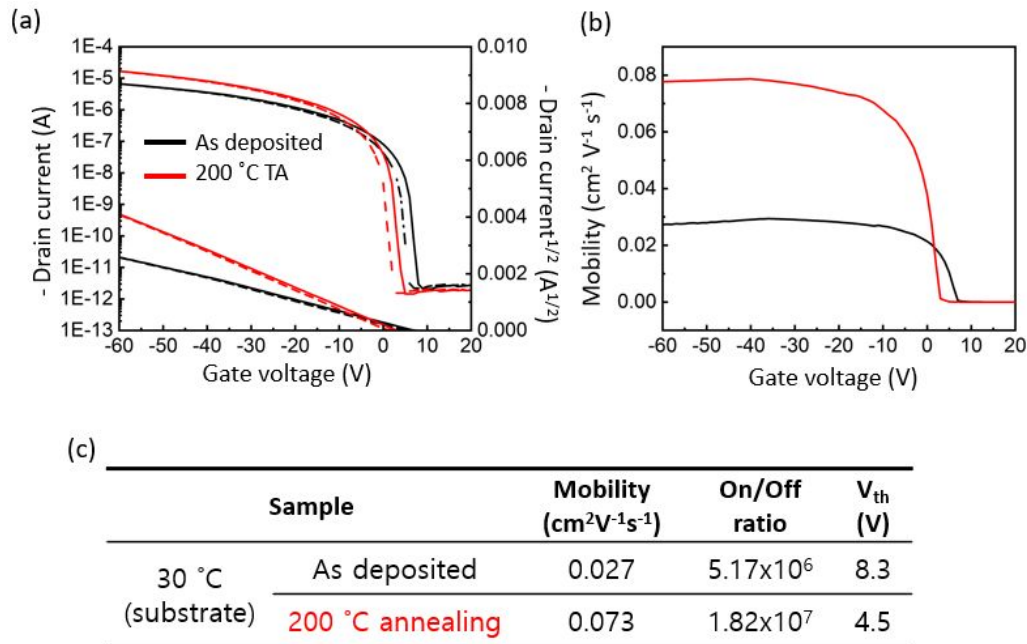


Figure S11. Electrical characterization of C12-Th-DBTTT film as thermally deposited at 30 °C and followed by 200 °C thermal annealing. (a) Transfer curves at saturation regime ($V_{DS} = -80$ V) (b) Mobility plotted in the saturation regimes as a function of gate bias, increasing bias direction. (c) Electrical characteristics of OTFTs.

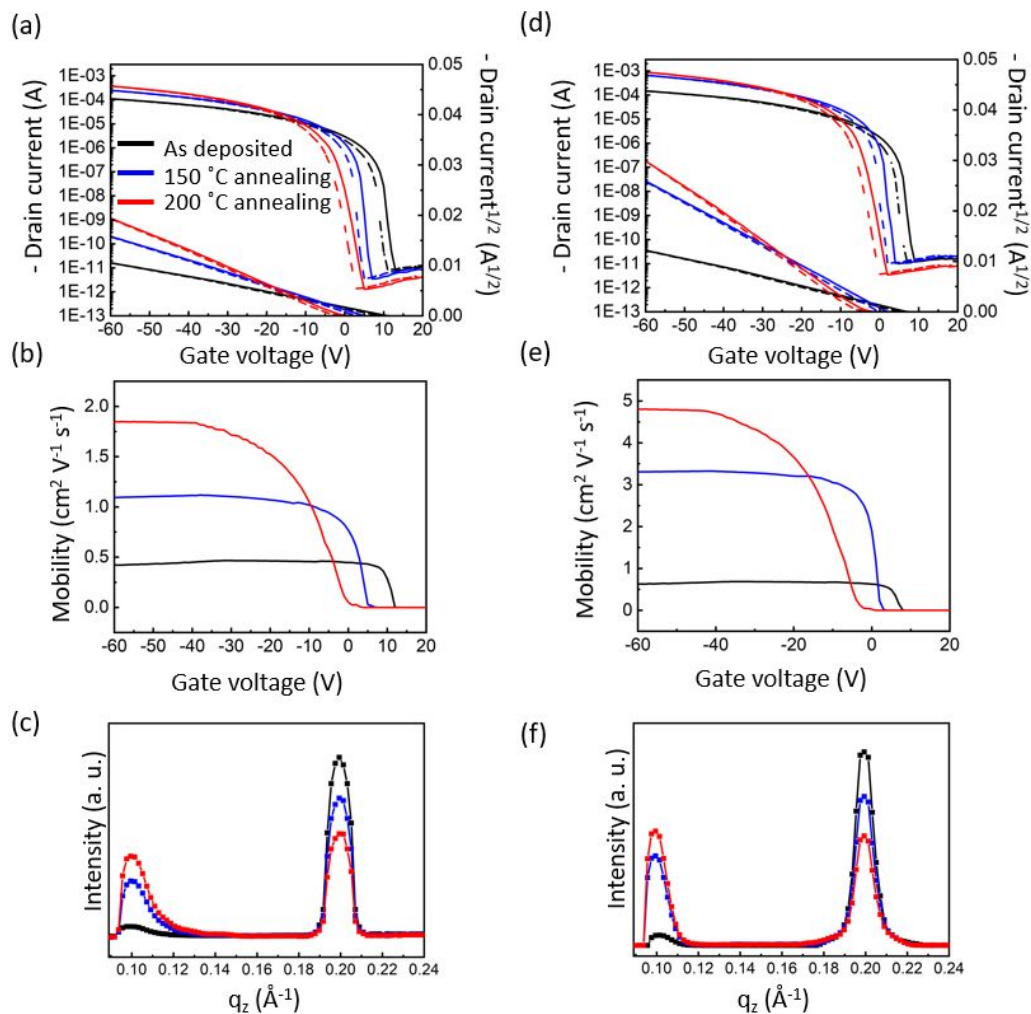


Figure S12. Molecular rearrangement characteristics depending on film fabrication temperature. Transfer characteristics at saturation regime with mobility as a function of gate voltage and out-of-plane small-angle XRD results of OTFTs based on crystalline films as-deposited at (a,b,c) 100 °C and (d,e,f) 135 °C followed by thermal annealing at 150 °C and 200 °C.

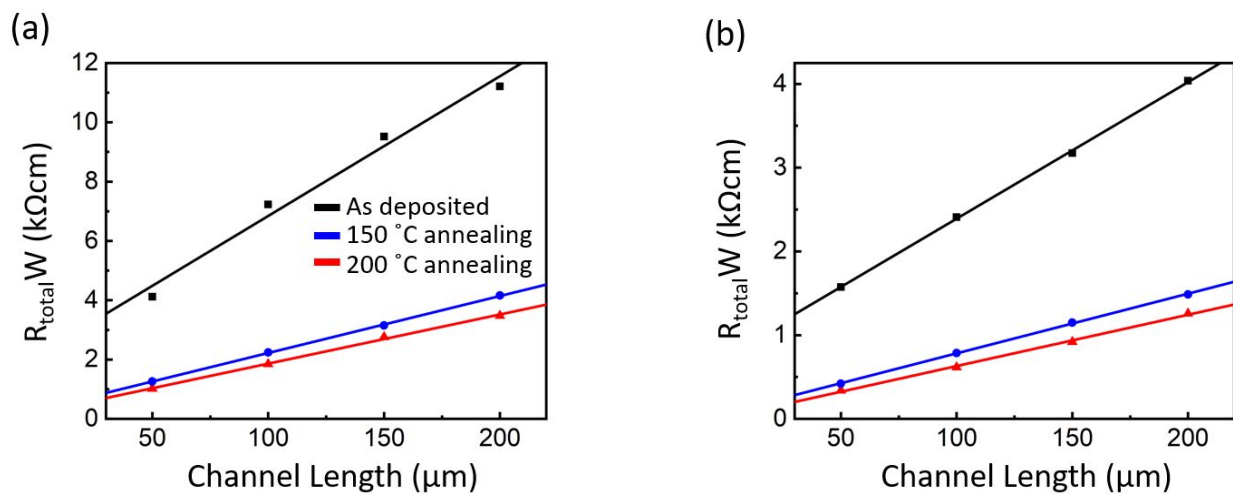


Figure S13. Contact resistance of OTFTs based on C12-Th-DBTTT films. (a) thermally deposited and (b) solution sheared at 165 °C followed by 150 °C and 200 °C thermal annealing. ($V_{\text{GS}} = -80 \text{ V}$)

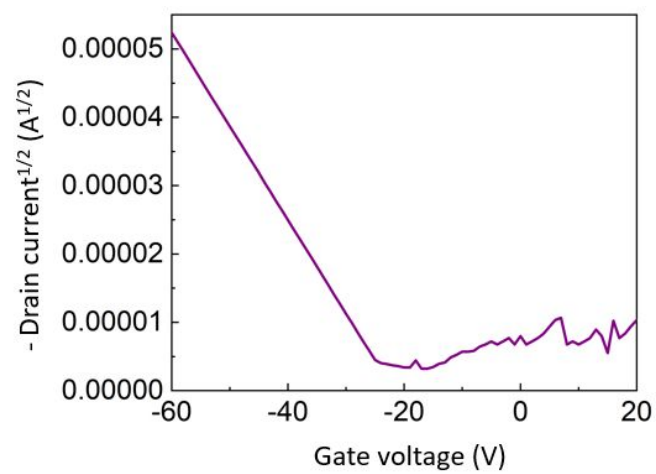


Figure S14. Transfer curve of C12-Th-DBTTT-based OTFT at 350 °C.

